International Journal of Fluid Power 5 (2004) No. 1 pp. 23-36

AN INVESTIGATION INTO MICRO- AND MACROGEOMETRIC DESIGN OF PISTON/CYLINDER ASSEMBLY OF SWASH PLATE MACHINES

Monika Ivantysynova and Rolf Lasaar

Technical University of Hamburg-Harburg, Institute for Aircraft Systems Engineering, Nesspriel 5, 21129 Hamburg, Germany
M.Ivantysynova@tuhh.de, Rolf.Lasaar@linde-mh.de

Abstract

This paper presents main results of an investigation of the tribological system formed by the piston/cylinder assembly of swash plate axial piston machines. Main focus has been given to the influence of a piston macro and micro geometry variation on energy dissipation generated by piston/cylinder assembly. Using the simulation tool *CASPAR*, which has been developed at the Institute for Aircraft Systems Engineering, an optimization of the piston shape has been realized to achieve minimum energy dissipation in a wide range of operating parameters of the axial piston machine. Micro geometry stands for surface roughness here. Its influence has been investigated within a second task especially in the area of low speed, where full lubrication is not achievable and therefore mixed friction occurs. For the investigation a special friction force measurement test rig has been developed, which has also been used for verification of the simulation tool *CASPAR*.

Keywords: axial piston machine, piston cylinder assembly, pressure field, friction force, gap flow, surface roughness, friction force measurement

1 Introduction

The achievable operating parameters, the loss behaviour and the reliability of displacement machines are mainly influenced by the design of the sealing and bearing gaps. Primary design parameters are, besides the choice of material, the micro and macro geometries of surfaces forming the gaps. Micro geometry denotes the surface quality and structure, whereas macro geometry stands for the dimensions of parts and shapes of surfaces forming the gaps surfaces. It should be mentioned here that pumps and motors can only achieve a relatively long service life when a sufficient lubricating film with an appropriate load carrying ability exists between the heavy loaded parts having relative motion to each other. Of course there are operating conditions of a pump or motor where full lubrication cannot be achieved, but such an unfavourable situation should only appear at very low speed or some other extremely high loading conditions. A well designed displacement machine has to run in a wide range of operating parameters without wear, i.e. mixed friction should be avoided.

The progress of production technologies, especially the improvement of possible accuracies, presently allows the designer to specify sophisticated macro geometries of parts, like e.g. a contoured piston shape with diameter differences in the range of a few microns and a certain curvature.

The aim of the reported research project was to investigate the influence of surface shape variations of parts forming the lubricating gap on gap flow parameters and energy dissipation, i.e. to investigate the potential for a further increase of operating parameters or improve of efficiency by optimization of gap design. Because full lubrication is not achievable in the whole range of operating parameters the influence of surface roughness was also of interest within the reported research work. The investigation was exemplarily made for the piston/cylinder assembly of a swash plate axial piston machine, Fig 1. The results can be transferred to other lubricating gaps as well.

Several investigations concerning the piston/cylinder assembly have been accomplished since the early 70s. Friction forces have been measured e.g. by Ezato Ikeya (1986), Kleist (2002), Manring (1999) and Tanaka (1999). The temperature behaviour has been investigated by Ivantysynova (1985) and Olems (2000), to name only a selection of the newer publications. All experimental works have in common, that the test devices are relatively simple one or two cylinder machines with inverse kinematics (rotating swash plate

This manuscript was received on 21 November and was accepted after revision for publication on 01 March 2004

and fixed cylinder block) in order to avoid problems, associated with data transfer from rotating components, except Olems, who measured the temperature field of the cylinder block for the first time at the rotating cylinder block and transferred data via telemetry. The advantages of such an arrangement are the consideration of centrifugal forces acting on the piston and the possibility to create a realistic instantaneous cylinder pressure during the revolution of the cylinder block. The same measurement strategy was chosen for the experimental work done within this project. This has finally allowed to measure piston friction forces under real operating conditions for many different piston shapes and roughnesses.

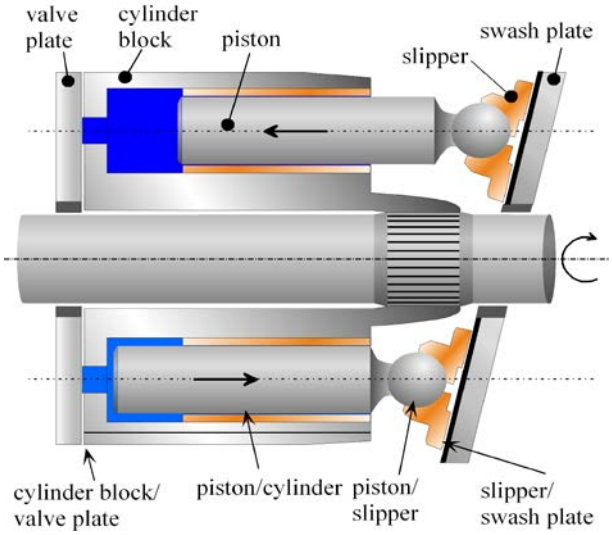

Fig. 1: *Gaps in swash plate machines*

For the theoretical investigations the gap flow simulation tool *CASPAR* has been used. *CASPAR* has been developed at the Institute for Aircraft Systems Engineering at Technical University of Hamburg-Harburg (Wieczorek and Ivantysynova, 2002) as a special software tool to assist and support the design and optimization of swash plate axial piston pumps and motors in a sophisticated way. *CASPAR* is based on a non-isothermal gap flow model considering the change of gap heights due to micro-motion of moveable parts (cylinder block, slipper and piston) and due to surface deformations for the connected gaps of a swash plate axial piston machine. The program allows the calculation of real flow ripple at the ports, further the calculation of the instantaneous cylinder pressure, pressure fields generated inside the gaps, the internal and external volumetric losses, viscous friction forces, gap heights and oscillating forces and moments exerted on the swash plate, see Ivantysynova et al (2002).

2 Influence of Piston Shape on Energy Dissipation

When studying the gap between piston and cylinder, first of all the forces exerted on the piston must be considered. Figure 2 shows a free body diagram of the piston for a certain angular position φ of the cylinder block. Assuming steady state conditions of the pump or motor all shown external forces are time dependent due to the pump kinematics and the instantaneous cylinder pressure, except the centrifugal force $F_{\omega K}$. These oscillating forces cause a micro-motion of the piston leading to time dependent gap heights and non-stationary gap flow even when the machine runs under steady state conditions. These are boundary conditions, which must be considered in the simulation model. The simulation program *CASPAR* calculates the oscillating pressure force F_{DK} by computing the instantaneous cylinder pressure p_D. Further the implemented non-isothermal gap flow model allows the calculation of the time dependent piston friction force F_{TK}, more details can be found in Wieczorek and Ivantysynova (2002). The mathematical model describing the non-isothermal gap flow, the micro-motion of the movable parts (piston, slipper and cylinder block) and the instantaneous cylinder pressure is solved numerically, where one revolution of the cylinder block is divided into a certain number of small time steps. Figure 3 shows exemplarily the gap between piston and cylinder for a given angular position of the cylinder block with the unwrapped gap in the $\hat{x}, \hat{y}$ plane. For each time step the pressure field generated by the gap flow can be obtained solving the non-isothermal gap flow model based on Reynolds-equation and energy equation. Figure 4 shows the calculated pressure field exemplarily for a given angular position of the cylinder block. The load carrying ability of the gap is given by:

$$F_{fK} = \int_0^{l_F} \int_0^{\pi d_K} p(\phi_K, z_K)\, d\phi_K\, dz_K\,, \tag{1}$$

where according to Fig. 3 for the transformation of the co-ordinate systems the following relationship is used:

$$\hat{x} = \frac{d_K}{2}\phi_K, \quad \hat{y} = z_K, \quad \hat{z} = h. \tag{2}$$

Figure 5 demonstrates the change of pressure fields between piston and cylinder for a cylindrical standard piston of a series machine during one shaft revolution. For space reasons the pressure field is plotted only for a few numbers of angular postions of the cylinder block. Using the calculated pressure field with the given pressure for each grid point $p_{i,j}$ the flow velocity in direction of gap circumference $\hat{x}$ can be obtained:

$$v_{\hat{x}}(\hat{z}) = u_K \cdot \frac{\hat{z}}{h} + \frac{1}{2\mu}\frac{\partial p}{\partial \hat{x}}(\hat{z}^2 - h\,\hat{z}) \tag{3}$$

The velocity u_K in Eq. 3 represents the relative circumferential velocity of the piston caused by the rotating cylinder block. This relative movement of the piston depends on the friction force between piston ball and slipper. The machine kinematics allows this additional degree of freedom of the piston movement; see Ivantysyn and Ivantysynova (2000). For the simulations performed in this paper $u_K = \omega \cdot d_K/2$.

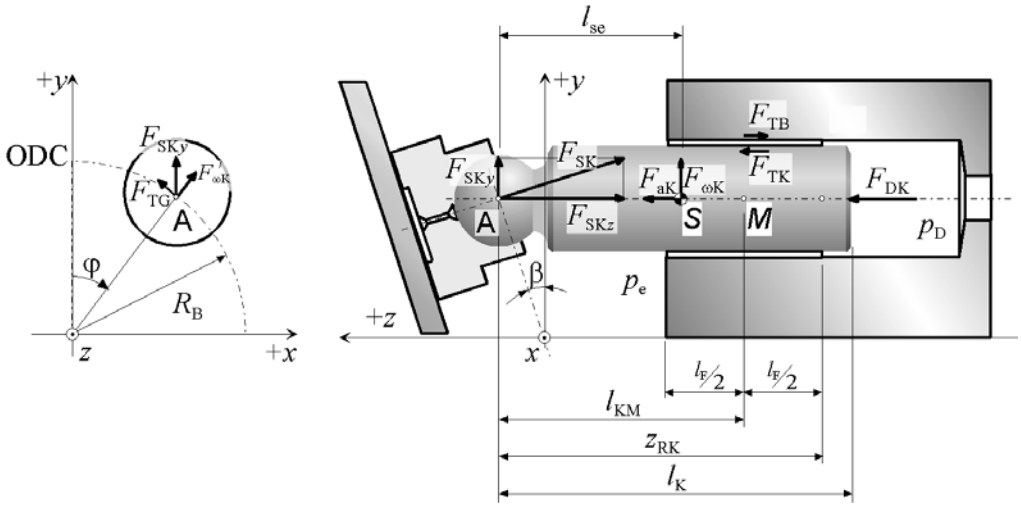

Fig. 2: *Forces acting on the piston*

The flow velocity in direction of gap length $\hat{y}$ yields:

$$v_{\hat{y}}(\hat{z}) = v_K \cdot \frac{\hat{z}}{h} + \frac{1}{2\mu}\frac{\partial p}{\partial \hat{y}}(\hat{z}^2 - h\,\hat{z}) \tag{4}$$

Using the derivative of flow velocity with respect to gap height z the shear stress can be calculated for each grid point:

$$\tau_{\hat{x}} = \mu \cdot \frac{\partial v_{\hat{x}}}{\partial z} = \mu \frac{u_K}{h} + \frac{\partial p}{\partial \hat{x}}\left(\hat{z} - \frac{h}{2}\right) \tag{5}$$

and

$$\tau_{\hat{y}} = \mu \cdot \frac{\partial v_{\hat{y}}}{\partial z} = \mu \frac{v_K}{h} + \frac{\partial p}{\partial \hat{y}}\left(\hat{z} - \frac{h}{2}\right) \tag{6}$$

The viscous friction force exerted on the piston in circumference direction yields:

$$F_{T,\tan} = \int_0^{\pi D_K} \int_0^{\hat{y}_{\max}} \tau_{\hat{x}}\, \mathrm{d}\hat{y}\, \mathrm{d}\hat{x} \tag{7}$$

and in direction of gap length:

$$F_{T,ax} = \int_0^{\pi D_K} \int_0^{\hat{y}_{\max}} \tau_{\hat{y}}\, \mathrm{d}\hat{y}\, \mathrm{d}\hat{x} \tag{8}$$

Figure 6 shows exemplarily simulation results obtained with *CASPAR* for the friction forces. The simulation was made for a swash plate axial piston machine with standard cylindrical pistons (S2 in Fig. 8) for pumping mode with a speed of 3000 rpm and 300 bar high pressure and 20 bar inlet pressure. As shown in Fig. 6, the friction force exerted on the cylinder surface is different from the piston friction force due to different gradients of flow velocities on both surfaces. This is important to consider when verifying the simulation results by measurements. The developed measurement device allows to measure only the friction force exerted on the bushing, see Fig. 12.

When optimizing the gap design besides the friction and load carrying ability of the gap also the gap flow is of interest. The flow from the displacement chamber through the gap into the case of the machine contributes to volumetric losses and must be kept as small as possible. The gap flow is given by:

$$Q_{\hat{y}} = \int_0^{\pi d_K} \int_0^{h} v_{\hat{y}}\, \mathrm{d}\hat{z}\, \mathrm{d}\hat{x} \tag{9}$$

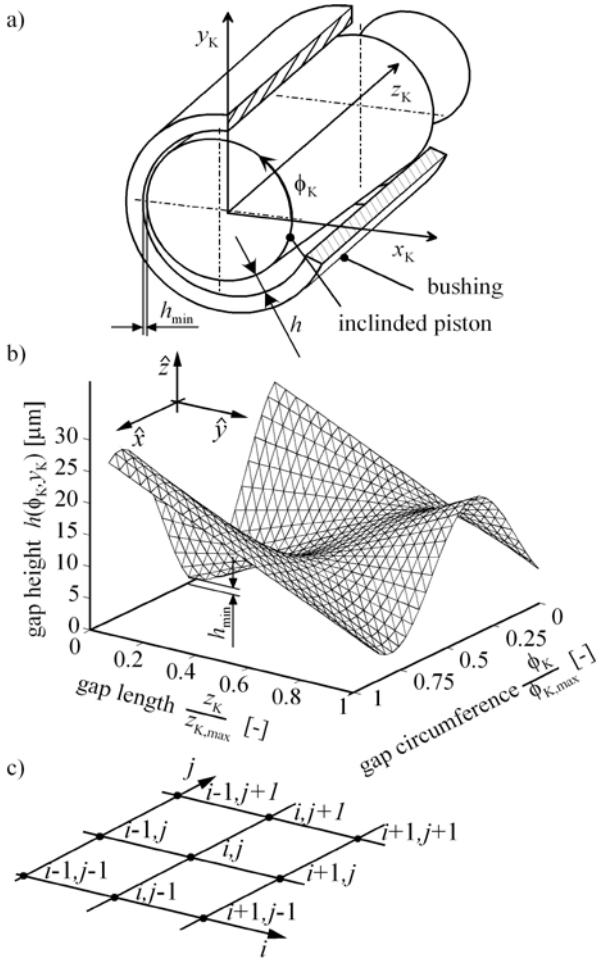

Fig. 3: *a) Inclined piston b) resulting gap heights, c) simulation grid*

Figure 7 shows exemplarily the calculated gap flow between piston and cylinder for the standard piston and the same operating parameters of the swash plate axial

piston pump. Positive values denote a flow from the displacement chamber into the case. The mean value of flow Q_{SK} flowing into the case during one shaft yields:

$$\overline{Q}_{SK} = \frac{1}{T}\int_0^T Q_{SK}\,dt\,, \qquad (10)$$

where T = time of shaft revolution.

For the given combination of operating parameters and the given small clearance in Fig. 7 (full line) the Couette flow dominates during the pumping phase, i.e. the flow flows from the case into the displacement chamber. The dotted line in Fig. 7 shows schematically how the flow through the gap changes with increasing clearance or pressure difference. Assuming same clearance and same speed the gap flow during pumping phase changes its direction with increasing operating pressure, i.e. the Poiseuille flow becomes larger and dominates the resulting flow direction. A similar effect is achieved with increasing clearance, but this will affect also the amount of flow during the suction phase. IDC denotes the inner dead point of the piston and ODC the outer dead point.

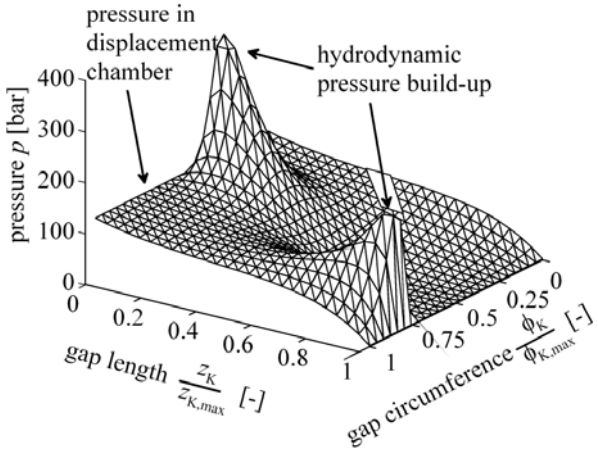

Fig. 4: *Pressure field inside the gap*

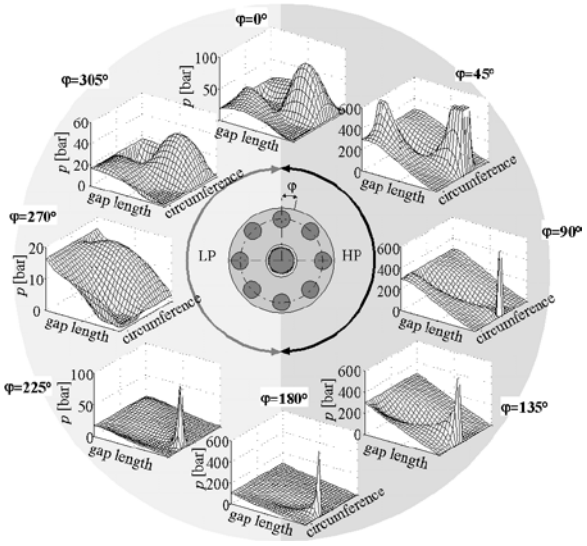

Fig. 5: *Pressure fields for different positions of the cylinder block calculated for a cylindrical piston with CASPAR for pumping mode, p_{HP}=300 bar, n=3000 rpm, ν=30 cSt, maximum swash plate angle*

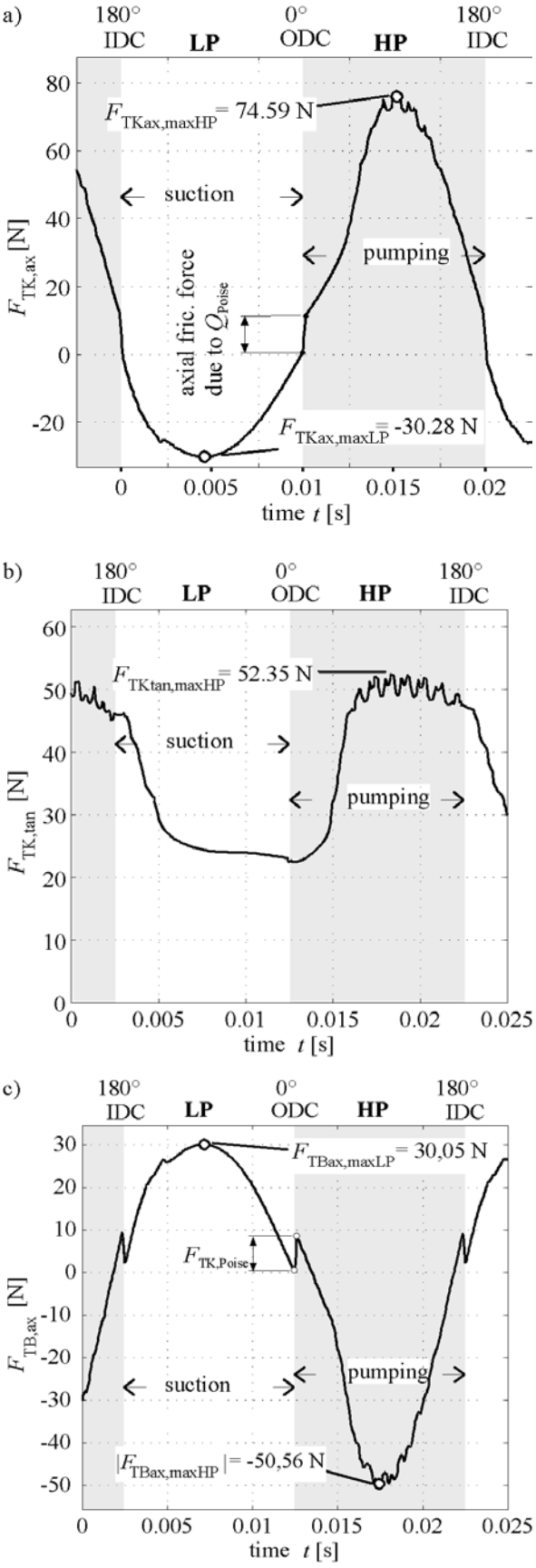

Fig. 6: *Simulated viscous friction forces a) axial direction/at the piston surface, b) tangential dir. /piston surface, c) axial dir. bushing surface (pumping mode, p_{HP}=300 bar, p_{LP}=20 bar, n=3000 rpm, ν=30 cSt, maximum swash plate angle)*

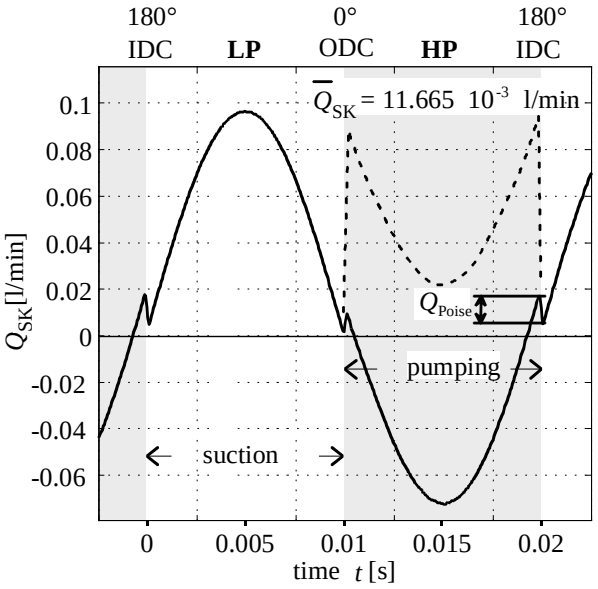

Fig. 7: *Simulated gap flow (pumping mode, p_{HP}=300 bar, p_{LP}=20 bar, n=3000 rpm, ν=30 cSt, maximum swash plate angle)*

2.1 The Optimized Piston Shape

Within the project a large number of different piston shapes has been analysed using the program *CASPAR* (Lasaar, 2003). For all investigated surface variations the load carrying ability, the piston friction force and the gap flow were computed for different operating parameters of a swash plate axial piston machine and compared with the standard cylindrical piston when running under same operating conditions. The investigations were made for pumping and motoring mode. The piston, which has performed best, i.e. has achieved the lowest energy dissipation in a wide range of operating parameters is shown in Fig. 8. It should be mentioned here that an optimization of piston shape for both pumping and motoring mode requires always a compromise, whereas the optimization of surface shape for only pumping mode or motoring mode respectively offers a much bigger potential for improvements.

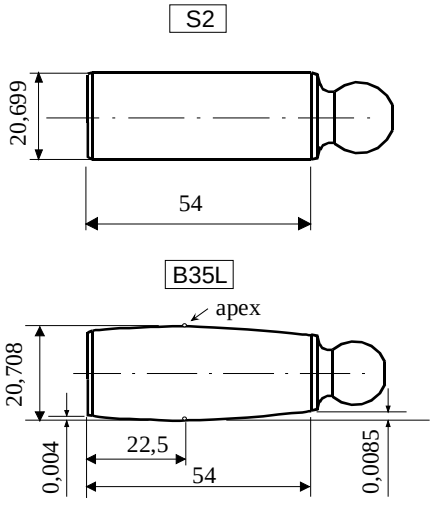

Fig 8: *Cylindrical and contoured piston geometries*

Figure 9 shows the calculated pressure field for the contoured piston B35L for again a certain number of angular positions of the cylinder block and the same operating parameters of the pump when running with standard pistons, see Fig. 5.

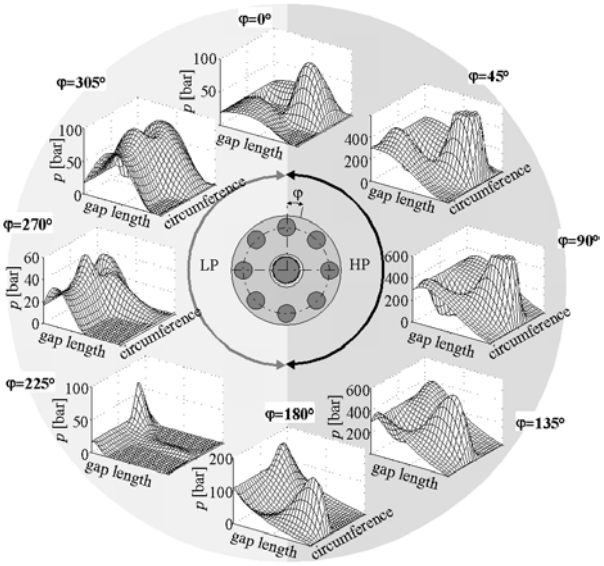

Fig. 9: *Pressure fields for different positions of the cylinder block calculated for the contoured piston B35L for pumping mode, p_{HP}=300 bar, n=3000 rpm, ν=30 cSt, maximum swash plate angle*

Using Eq. 7 and Eq. 8 the resulting friction force yields:

$$F_{TKall} = \sqrt{F_{TKax}^2 + F_{TKtan}^2} \tag{11}$$

Figure 10 shows the resulting piston friction forces for the contoured piston B35L and the standard piston S2, plotted over one shaft revolution.

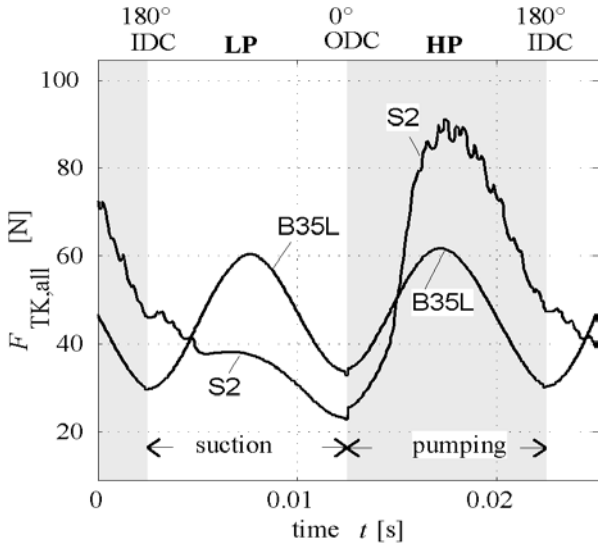

Fig. 10: *Resulting viscous friction forces (pumping mode, p_{HP}=300 bar, p_{LP}=20 bar, n=3000 rpm, ν=30 cSt, maximum swash plate angle)*

Figure 11 shows the simulation result for the gap flow for both pistons. It is obvious that this piston helps to reduce torque losses and volumetric losses of the pump.

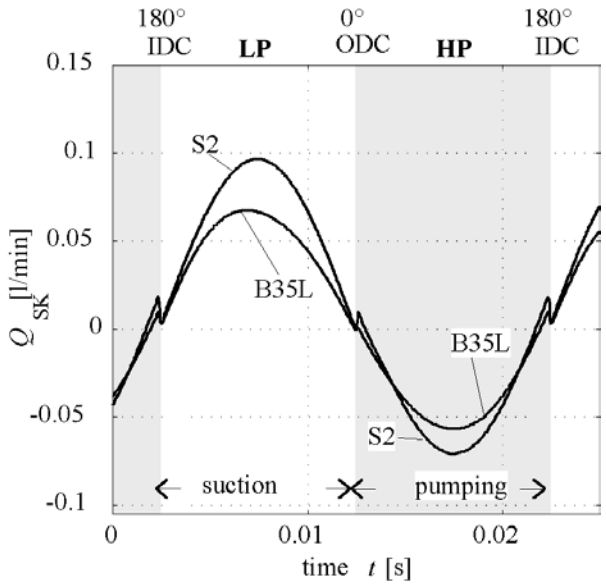

Fig. 11: *Gap flow for both pistons plotted over one shaft revolution (pumping mode, p_{HP}=300 bar, p_{LP}=20 bar, n=3000 rpm, ν=30 cSt, maximum swash plate angle)*

Simulation results obtained with *CASPAR* have been verified by experiment. For this purpose a special test rig was developed and built at the Institute for Aircraft Systems Engineering.

3 Friction Force Measurement

3.1 The Measurement Device

The aim of the measurement device shown in Fig. 12, which is also called *tribo pump*, is the realization of friction force measurements on the piston/cylinder assembly under conditions and operating parameters comparable with series swash plate axial piston machines. The friction force measurements were made to verify the simulation results, to investigate the behaviour of contoured pistons at low speed, i.e. in an area where full lubrication cannot be achieved, and to investigate the influence of micro geometry of surfaces forming the lubricating gap.

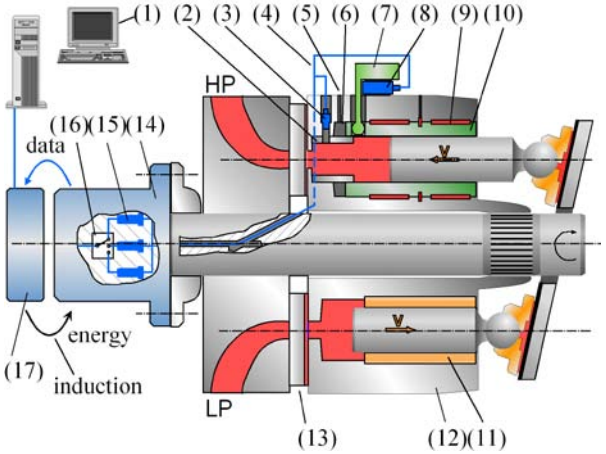

Fig. 12: *Tribo pump measurement principle*

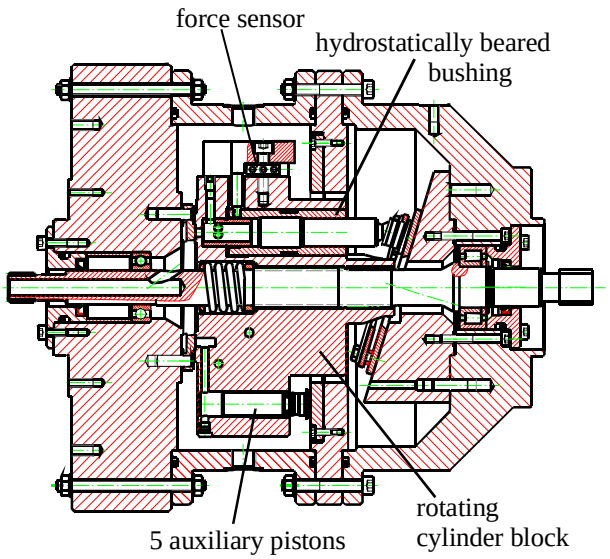

Fig. 13: *Tribo pump – cross section*

The proposed test pump design is schematically shown in Fig. 12. To measure the friction force at the piston/cylinder assembly on the rotating cylinder block the standard bushing (11), which is pressed into the cylinder block has been replaced by a hydrostatically beared bushing (10). A three axes piezoelectric force sensor is connected via a lever arm (7) with the bushing (10) and has been used for measurement of friction forces applied on the cylinder bushing. A piezoelectric pressure sensor (4) has been used for measurement of instantaneous cylinder pressure. To guarantee comparable conditions between simulation and measurement *CASPAR* allows reading measured pressure signals as input data. As mentioned before *CASPAR* can also calculate the instantaneous pressure by reading the valve plate geometry, but when reading a measured pressure profile directly, the calculated gap flow parameters should fit best. To achieve the highest possible level of comparability with standard machines the piston pitch diameter, the diameter of the bushing, the piston stroke as well as the slipper and valve plate design were made identically to a standard machine. For space reason the *tribo pump* has only three active pistons. For balancing the cylinder block five auxiliary pistons were necessary, which are supported by a part of the housing as shown in Fig. 13 and in the 3D cross section in Fig. 14.

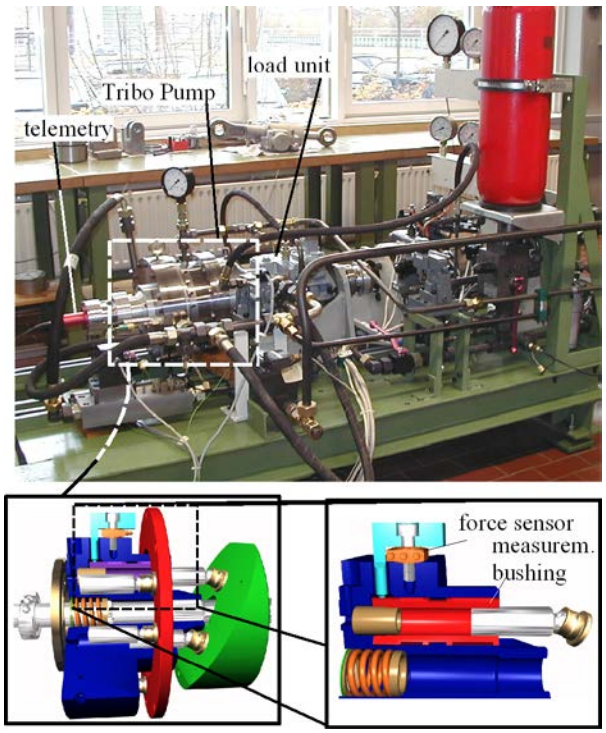

Fig. 14: *Tribo test rig*

3.2 Exemplary Measurement Results

The test rig allows to measure friction forces applied on the bushing in axial and circumferential (tangential) direction. Figure 15 shows exemplarily measurement results obtained for a standard piston mounted into the *tribo pump* when running in pumping mode at 1000 rpm and 100 bar pressure difference. For the measurement of friction forces applied on the bushing in circumferential direction, i.e. the friction force due to relative rotation of the piston, it was not possible to obtain absolute values. The reason for that is given by the piezo electric sensor principle of the applied force sensor, which does not allow to measure static values, but is suitable for measurement of dynamic forces. To obtain absolute values the sensor needs to be calibrated. The calibration for the measurement of axial friction forces was made by using the inner and outer deadpoint of the piston to define the zero point. In the case of the tangential friction force measurement the zero point could not be found. Because for the relative piston rotation causing tangential friction forces a standstill of the piston is not easy to define.

That's why Fig. 15 b shows only the scaling with the value corresponding to 5 N, but not an absolute value of the measured friction force.

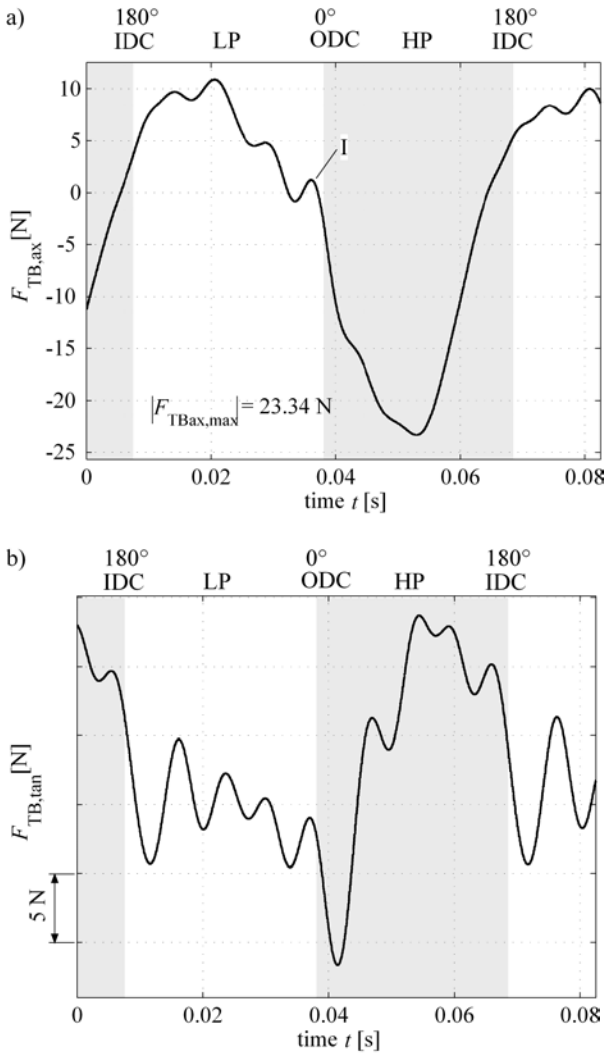

Fig. 15: *Measured friction forces between piston and cylinder a) axial direction, b) tangential direction (pumping mode, p_{HP}=120 bar, p_{LP}=18 bar, n=1000 rpm, ν=30 cSt, maximum swash plate angle, ω_{Filter}=140 Hz, piston S2)*

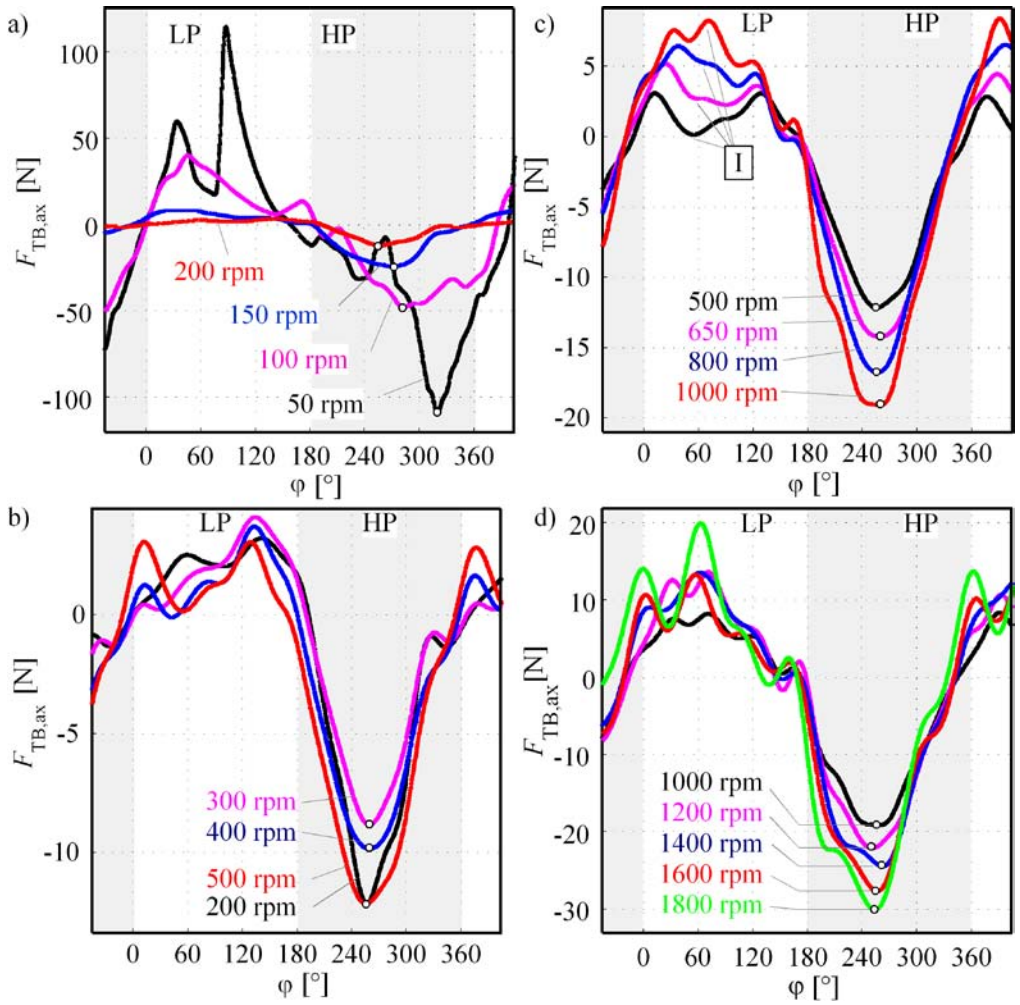

Fig. 16: *Measured axial friction forces for standard piston S2 (pumping mode, p_{HP}=80 bar, ν=30 cSt, maximum swash plate angle, a) 50-200rpm, b) 200-500 rpm, c) 500-1000rpm, d) 1000-1800rpm)*

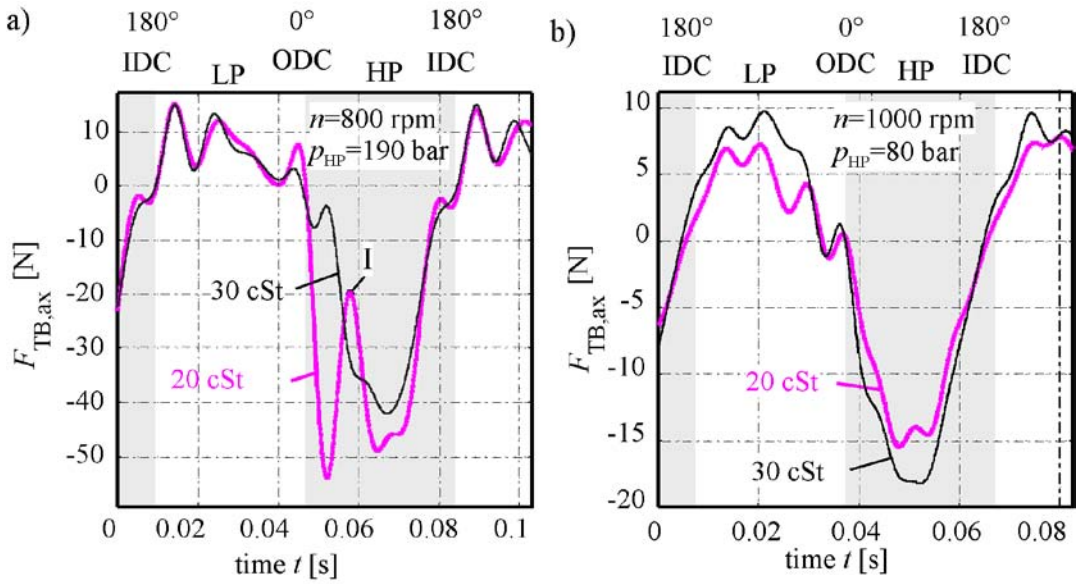

Fig. 17: *Measured axial friction forces for two different temperatures or viscosities resp. (pumping mode, p_{LP}=18 bar, β=17°, piston S2, a) p_{HP}=190 bar, n=800 rpm, b) p_{HP}=80 bar, n=1000 rpm)*

Figure 16 shows a series of measurement results obtained again for the standard piston S2 in pumping mode for different pump speeds starting with 50 rpm up to 1800 rpm. During all measurements the input temperature of the oil was kept constant at 42°C. For the used oil HLP 32 this corresponds to a kinematic viscosity of 30 cSt. Figure 17 demonstrates the influence of viscosity on the tribological behaviour of piston/-cylinder assembly. Friction force measurements were made for the same cylindrical piston S2 for two different operating parameters and two different oil temperatures at the pump inlet corresponding to 20 cSt and 30 cSt. The graph on the right side of Fig. 17 shows a condition where at 1000 rpm and 80 bar high pressure full lubrication is achieved. The graph on the left side shows measured friction forces for 800 rpm pump speed and 190 bar high pressure where the load carrying ability of the gap becomes a critical issue. Especially the friction force curve for lower viscosity (20 cSt) shows clearly that the piston after crossing its outer dead point is not sufficiently balanced by fluid forces and mixed friction appears.

3.3 Comparison of Simulated and Measured Friction Forces for the Standard Piston

In case of full lubrication conditions the simulated piston friction forces should fit with the measured values. Figure 18 shows exemplarily a comparison of axial friction forces obtained with the standard *CASPAR* version assuming rigid parts a) and simulation results obtained with an extended program version, where also elastohydrodynamic effects (EHD) are considered b), see also (Ivantysynova and Huang, 2002 and 2003). Figure 18c) shows measured friction forces for two pressure levels. It is obvious from Fig. 18d) that the EHD model fits better with measurements, especially on the high pressure side.

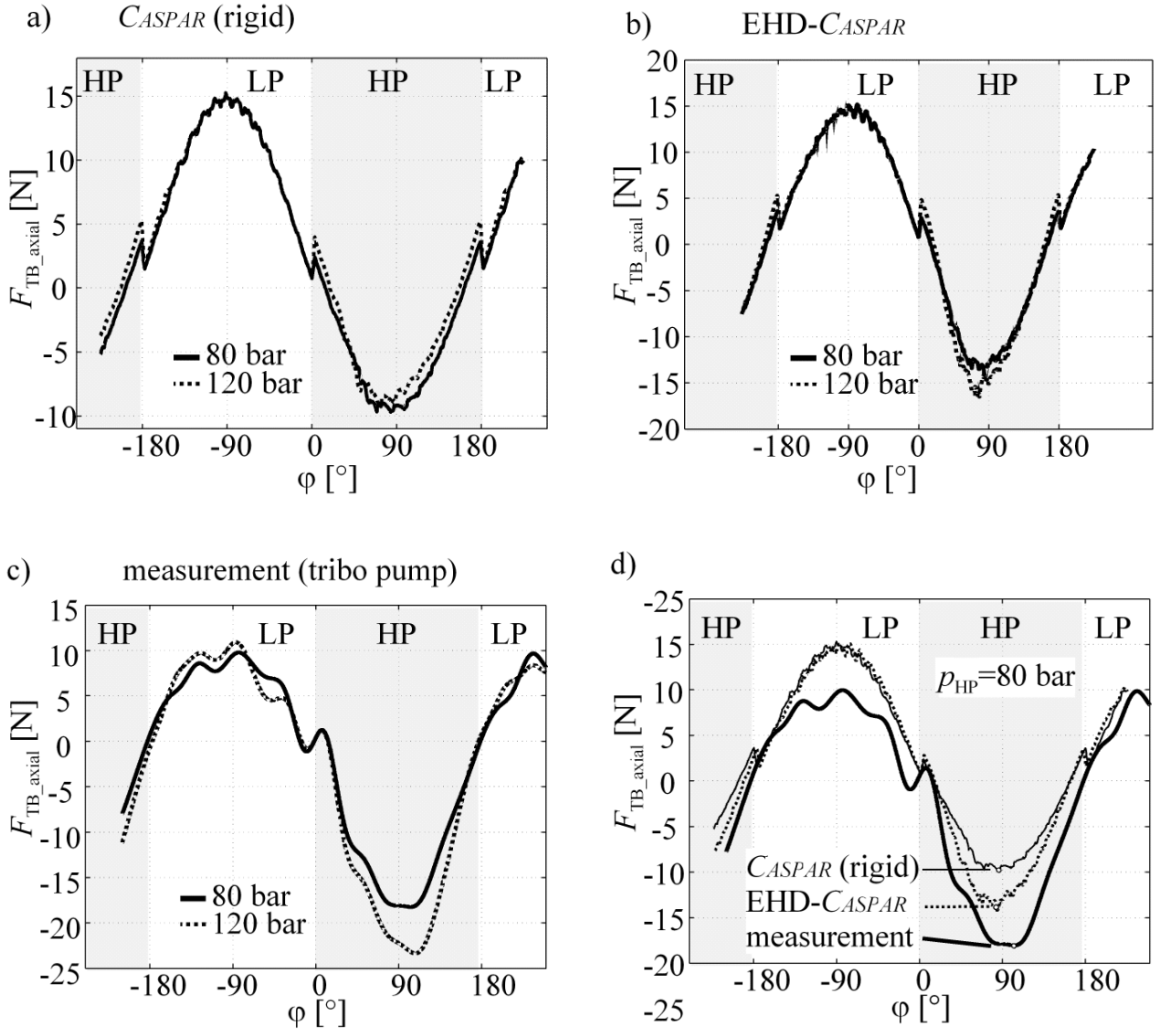

Fig 18: *Comparison of simulated and measured axial friction forces for two pressure levels a) rigid CASPAR version, b) EHD CASPAR version, c) measurement d) all in one diagram (pumping mode, n=1000 rpm, p_{LP}=18 bar, p_{HP}=80/120 bar, ν=30 cSt, standard piston S2 and maximum swash plate angle)*

Figure 19 shows a comparison of tangential friction forces with simulation results again for both program versions and measured values for two pressure levels. As mentioned before the measurement of tangential friction forces had not allowed determining absolute values. But the shape of the measured and simulated friction curves fits relatively well.

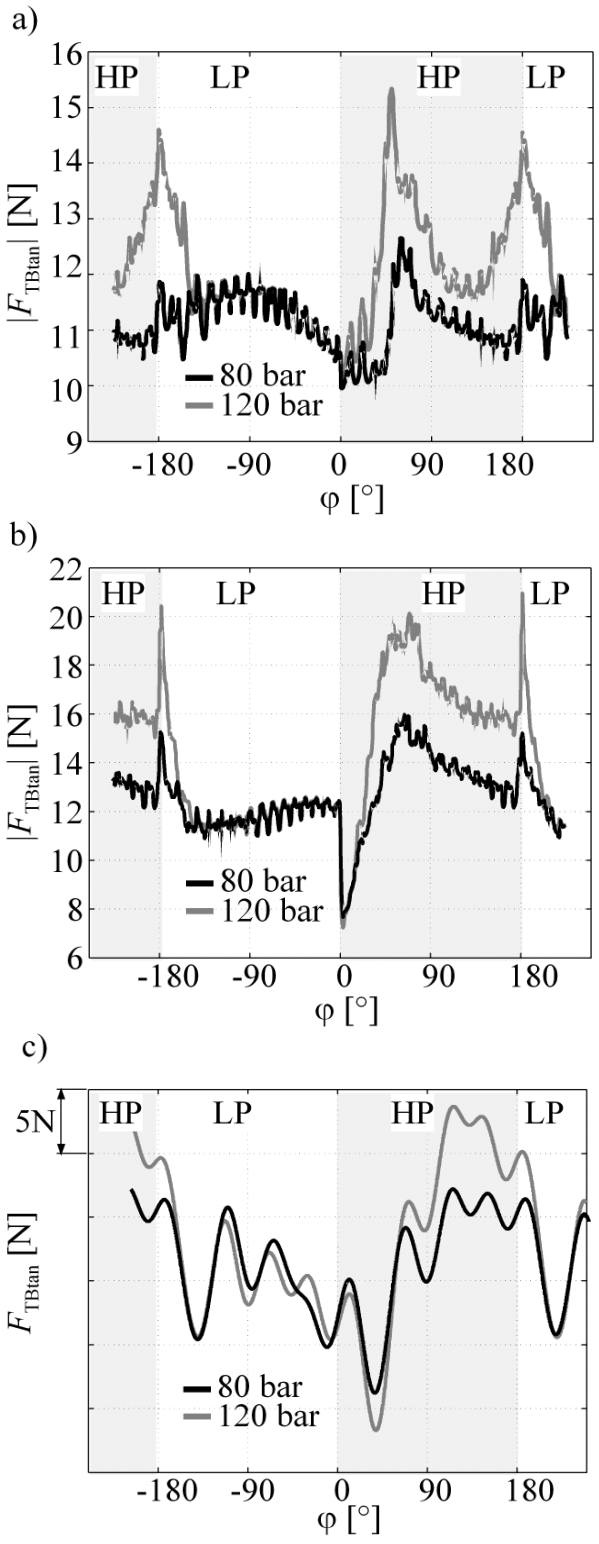

Fig 19: *Comparison of simulated and measured tangential friction forces for two pressure levels a) rigid CASPAR version, b) EHD CASPAR version, c) measurement (pumping mode, n=1000 rpm, p_{LP}=18 bar, p_{HP}=80/120 bar, n=30 cSt)*

3.4 Measured Friction Forces on the Contoured Piston

Figure 20 shows the dimensions of a contoured piston, which was manufactured by high precision hard turning. This piston HB1 has a shape very similar to the piston B35L with an optimized shape found by *CASPAR* simulation runs. Compared to today's standard piston production process *grinding*, the hard turning process leads to a different surface micro structure even for the same values of arithmetical mean surface roughness. To eliminate effects caused by the different surface finishing a cylindrical piston with dimensions of the standard piston S2 was manufactured by hard turning. This cylindrical piston H6 has a similar value of arithmetical mean surface roughness as the contoured piston HB1. This had allowed to investigate the influence of surface shape on friction forces in a wide range of operating parameters, i.e. also in the area of mixed friction.

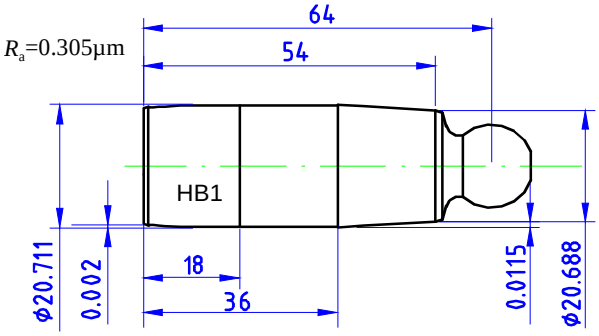

Fig. 20: *Macro geometry of piston HB1*

Figure 21 shows a comparison of measured friction forces for the cylindrical piston H6 and the contoured piston HB1 for different pressures at a pump speed of 500 rpm and an inlet temperature corresponding to 30 cSt. Both pistons are manufactured by high precision hard turning. The contoured piston HB1 has an arithmetical mean surface roughness of 0.305 µm. The value of the cylindrical piston H6 is given in Table 1. When comparing the friction force curves measured for the contoured piston and the cylindrical piston shown in Fig. 21 it is obvious that the contoured piston improves the load carrying ability. At higher pressures (190 bar) the cylindrical piston starts to run under mixed friction, whereas the contoured piston still achieves full lubrication. Figure 22 shows that improvements were also achieved for motoring mode.

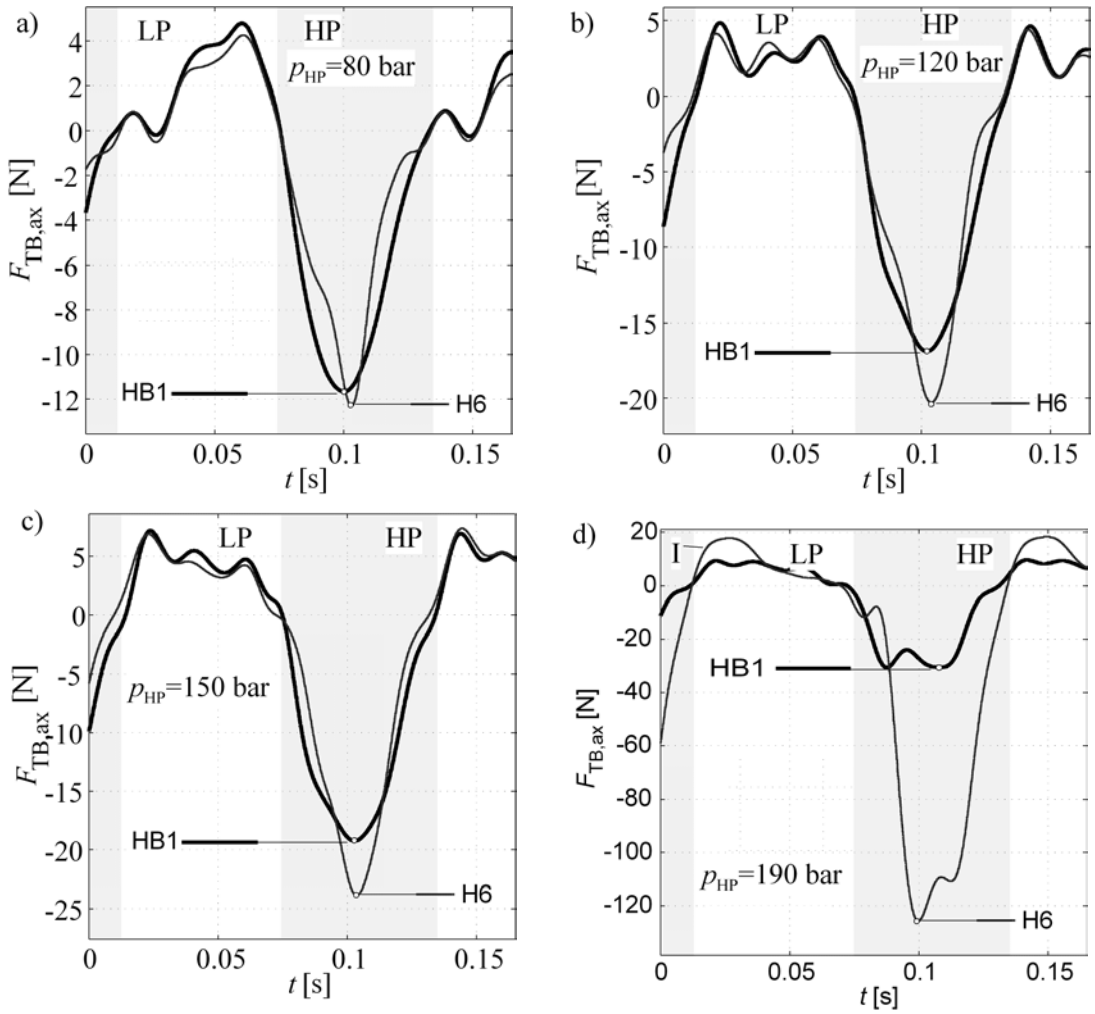

Fig. 21: *Macro geometry influence on friction forces pumping mode, n=500 rpm, p_{LP}=18 bar, ν=30 cSt a) p_{HP}=80 bar, b) p_{HP}=120 bar, c) p_{HP}=150 bar, d) p_{HP}=190 bar*

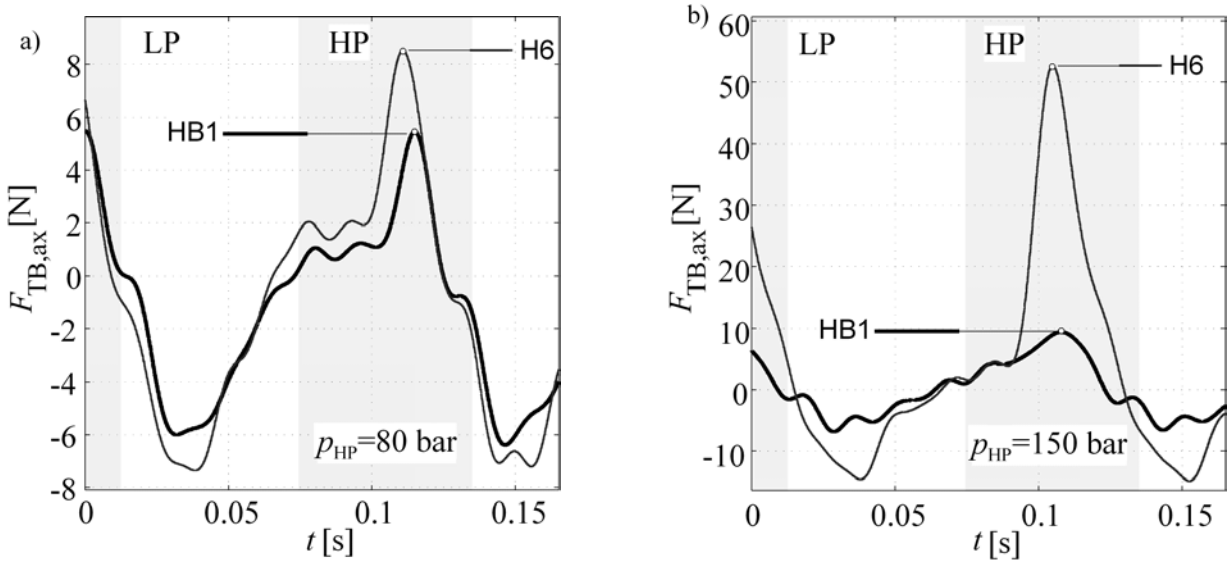

Fig. 22: *Macro geometry influence on friction forces, motoring mode, n=500 rpm, p_{LP}=18 bar, ν=30 cSt, a) p_{HP}=80 bar, b) p_{HP}=150 bar*

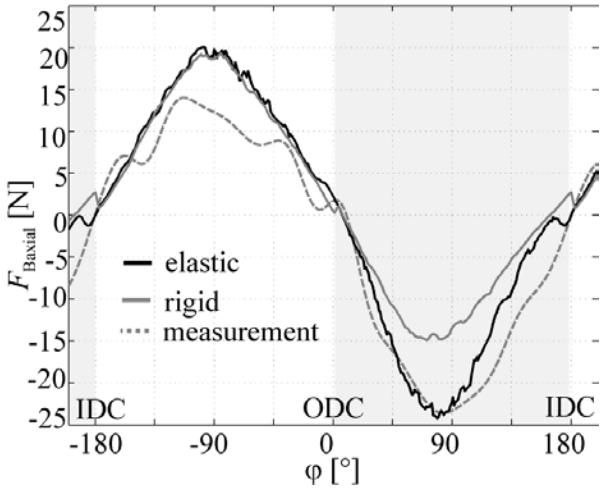

Fig. 23: *Comparison of measured and simulated friction forces for the contoured piston HB1, n=1000 rpm, p_{LP}=18 bar, p_{HP}=120 bar, ν=30 cSt, pumping mode*

Figure 23 shows a comparison of simulated and measured piston friction forces for the contoured piston HB1 for a pump speed of 1000 rpm and 120 bar high pressure and a corresponding inlet temperature of 42°C (ν=30 cSt). The full blackline shows the calculated friction force obtained on the bushing surface using the EHD CASPAR version. It is obvious that the elasto-hydrodynamic simulation model fits better with the measured friction force, especially during the high pressure phase. During suction stroke both simulation models gives higher pressure forces than the measurement. The authors do not have any explanation for this effect at the moment.

4 Micro Geometry Influence

A second topic of the reported research project was the investigation of the influence of surface roughness on energy dissipation in the gap. Because of missing generally valid analytical models for description of physical effects taking place during mixed friction the *CASPAR* simulation does not include any mixed friction model. With *CASPAR* only conditions with full lubrication can be computed. Therefore the investigation of micro geometry was realized experimentally using the friction force measurement device presented in section 3. Seven cylindrical pistons with nearly the same diameter as the standard piston S2 were made and mounted into the tribo pump. The pistons had a different arithmetical mean roughness value, which was measured before the test runs, see Table 1. All pistons are made from hardened steel. Pistons H1, H2, H3 and H6 were produced by high precision hard turning. The pistons P1 and P2 were polished after grinding and achieved a much better surface quality than the standard piston. For all measurements a brass bushing with diameter and roughness given in the last column (MB) of Table 1 was used.

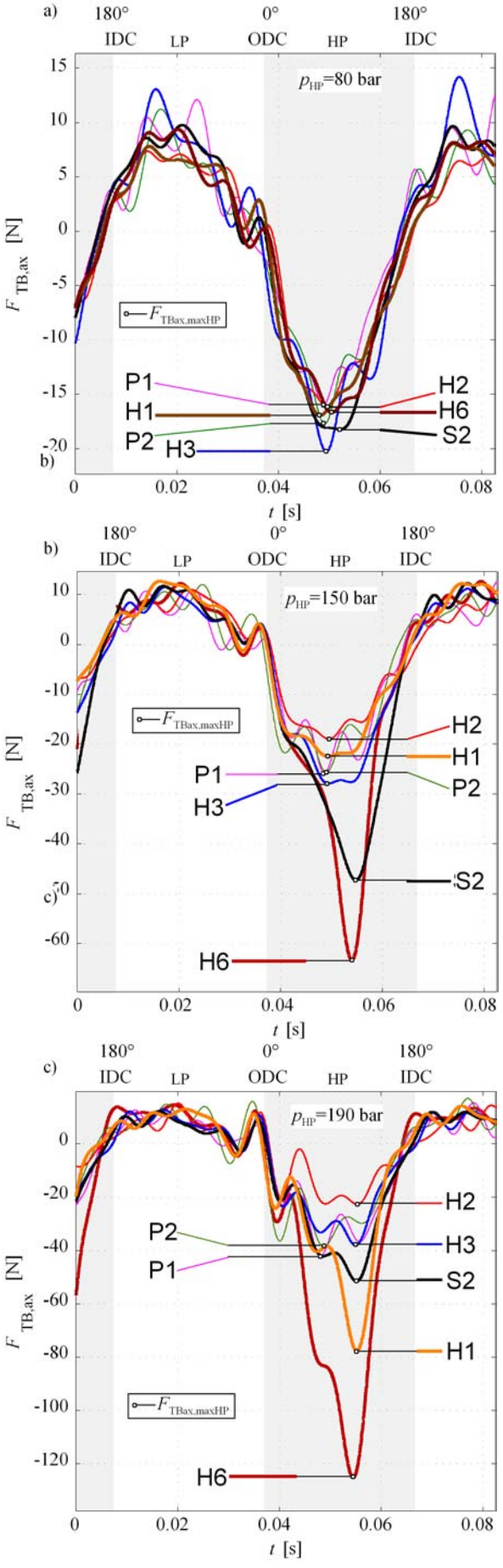

Fig. 24: *Micro geometry influence (pumping mode, n=1000 rpm, p_{LP}=18 bar, ν=30 cSt a) p_{HP}=80 bar, b) p_{HP}=150 bar, c) p_{HP}=190 bar)*

Figure 24 shows measured friction forces for all tested pistons for different high pressures. All measurements shown in Fig. 24 were made for pumping mode at a pump speed of 1000 rpm and with an inlet temperature kept constant at 42°C (30 cSt). The measured friction force curves show clearly the dependence on surface finish. The results show further that a too high quality (extremely low arithmetical mean roughness) of the surface does not contribute to a further decrease of friction. The piston H2 made by high precision hard turning has achieved the lowest friction. This can be explained by the different surface structure. The hard turning process produces a micro geometry with grooves, which when filled with oil can help to reduce mixed friction forces. The measurements confirm the recommendations one can find in literature that an arithmetical mean roughness of approx. 0.1 µm represents the optimal value for this kind of tribological system.

Table 1: micro geometries of pistons and bushing

part	**P1**	**P2**	**H2**	**H3**	**S2**	**H1**	**H6**	**MB**
R_a [µm]	0.004	0.024	0.07	0.1	0.114	0.208	0.35	1.194
d_K [mm]	20.697	20.697	20.703	20.703	20.699	20.703	20.699	20.724
s_{rel} [-]	1.303	1.303	1.013	1.013	1.206	1.013	1.206	

5 Conclusion

This paper demonstrates the potential of an advanced gap design using computer simulation. The presented contoured piston shape has been found by model based optimization. Here the program *CASPAR*, which was developed at the Institute for Aircraft Systems Engineering, was used. This program includes a non-isothermal gap flow model, which is solved numerically for the connected gaps of swash plate axial piston machines. Especially the oscillating forces lead to micro-motion of moveable parts, which has to be considered when computing the gap flow in individual gaps. A modified version of the program *CASPAR* allows considering elasto-hydrodynamic forces. A comparison of simulated and measured friction forces has shown that the EHD model fits better with measurements. The contoured piston improves the load carrying ability of the gap and allows reducing both volumetric losses and torque losses of the machine. The measurements have also shown that a shaped piston can contribute to an extension of the operating parameter range where full lubrication is achieved. Finally the experimental investigations of micro geometry have confirmed that it is not necessary to polish surfaces of lubricating gaps of displacement machines.

Nomenclature

d_K	piston diameter	[mm]
F_{aK}	inertia force of of piston	[N]
F_{AK}	axial piston force	[N]
F_{DK}	pressure force on piston	[N]
F_{fK}	fluid force	[N]
F_{SK}	reaction force swash plate	[N]
F_T	friction force	[N]
F_{TB}	friction force on bushing surface	[N]
F_{TG}	slipper friction force	[N]
F_{TK}	piston friction force	[N]
$F_{\omega K}$	centrifugal force on piston	[N]
h	gap height	[µm]
H_K	piston stroke	[mm]
IDC	inner dead centre	[-]
l_F	piston guide length	[m]
n	shaft speed	[rpm]
ODC	outer dead centre	[-]
p	pressure	[bar]
p_D	pressure in cylinder chamber	[bar]
p_e	housing pressure	[bar]
p_{HP} (HP)	high pressure level	[bar]
P_{LP} (LP)	low pressure level	[bar]
Q_{SK}	gap flow (piston/cylinder)	[l/min]
$\overline{Q}_{SK}$	mean gap flow	[l/min]
R_B	pitch diameter	[mm]
s_{rel}	relative clearance	[-]
t	time	[s]
T	oil temperature	[K]
u_K	relative circumferential speed of the piston	[m/s]
v_K	piston velocity	[m/s]
x, y, z	Cartesian co-ordinates	[mm]
$\hat{x}, \hat{y}, \hat{z}$	co-ordinates (unwrapped gap)	[mm]
β	swash plate angle	[°]
φ	rotating angle	[°]
µ	dynamic viscosity	[Pa s]
ρ	density	[kg/m^3]
ν	kinematical viscosity	[cSt]
ω	angular velocity	[rad/s]
ω_{Filter}	3dB-frequency of the low pass filter	[Hz]

References

Ezato, M. and **Ikeya, M.** 1986. Sliding Friction Characteristics between a Piston and a Cylinder Starting and Low-Speed Conditions in the Swashplate-Type Axial Piston Motor. *7th International Fluid Power Symposium*, Bath, UK.

Fang, Y. and **Shirakashi, M.** 1995. Mixed lubrication characteristics between the piston and cylinder in hydraulic piston pump-motor. *ASME Transactions, Journal of Tribology*, vol. 117, pp. 80-85.

Ivantysynova, M. 1999. Ways for Efficiency Improvements of Modern Displacement Machines. *Proc. of*

the Sixth Scandinavian International Conference on Fluid Power, Tampere, Finland, pp.77-92.

Ivantysynova, M. 1999. A new approach to the design of sealing and bearing gaps of displacement machines. *Proc. JHPS International Symposium on Fluid Power*, Tokyo, Japan.

Ivantysyn, J. and **Ivantysynova, M.** 2000. *Hydrostatic Pumps and Motors, Principles, Designs, Performance, Modelling, Analysis, Control and Testing.* Academia Books International, New Delhi. (ISBN - 81-85522-16-2)

Ivantysynova, M.; Grabbel, J. and **Ossyra, J.-C.** 2002. Prediction of Swash Plate Moment Using the Simulation Tool CASPAR. *2002 International Mechanical Engineering Congress and Exposition*, IMECE2002-39322, New Orleans, Louisiana, USA.

Ivantysynova, M. and **Huang, C.** 2002. Investigation of the Gap Flow in Displacement Machines Considering Elastohydrodynamic Effect. *2002 The Fifth JFPS International Symposium on Fluid Power, Nara 2002*. Nara, Japan.

Kleist, A. 1997. Design of hydrostatic bearing and sealing gaps in hydraulic machines- A new simulation tool. *Proc. of the 5th Scandinavian International Conference on Fluid Power ICFP*, Linköping, Sweden, pp. 157-169.

Kleist, A. 2002. *Berechnung von Dicht- und Lagerfugen in hydrostatischen Maschinen.* Institute for Fluid Power Drives and Controls (IFAS), University of Aachen (RWTH), Aachen, Germany, Shaker Verlag Aachen, ISBN 3-8322-0279-X.

Lasaar, R. 2000. The influence of the microscopic and macroscopic gap geometry on the energy dissipation in the lubricating gaps of displacement machines. *Proc. of 1st FPNI-PhD Symposium Hamburg 2000*, ISBN 3-00-006510-5, Hamburg, Germany, pp. 101-116.

Lasaar, R. and **Ivantysynova, M.** 2001. Gap geometry variations in displacement machines and their effect on the energy dissipation. *Proc. of the 5th International Conference on Fluid Power Transmission and Control*, Hangzhou, China, pp. 316-322.

Lasaar, R. and **Ivantysynova, M.** 2002. Advanced gap design – basis for innovative displacement machines. *Proc. of 3rd IFK (Internationales Fluidtechnisches Kolloquium)*, ISBN 3-8265-9901-2, Aachen, Germany, pp. 215-230.

Lasaar, R. 2003. *Eine Untersuchung zur mikro- und makrogeometrischen Gestaltung der Kolben/-Zylinderbaugruppe von Schrägscheibenmaschinen.* Dissertation TU Hamburg-Harburg, ISBN 3-18-336401-8, VDI-Verlag, Düsseldorf.

Manring, N. D. 1999. Friction forces within the cylinder bores of swash-plate type axial-poston pumps and motors. *Journal of dynamic systems, measurement and control*, Vol. 121, pp. 531-537.

Olems, L. 2000. Investigations of the temperature behaviour of the piston cylinder assembly in axial piston pumps. *International Journal of Fluid Power*, Vol. 1, No.1, pp. 27-38.

Renius, K. T. 1974. Untersuchungen zur Reibung zwischen Kolben und Zylinder bei Schräg-scheiben-Axialkolbenmaschinen. *VDI Forschungsheft 561*, Düsseldorf: VDI-Verlag.

Tanaka K.; Kyogoku K. and **Nakahara, T.** 1999. Lubrication characteristics on sliding surfaces between piston and cylinder in a piston pump and motor (Effects of running-in, profile of piston top and stiffness). *JSME International Journal, Series C (Mechanical Systems, Machine Elements and Manufacturing)*, Vol. 42, No. 4, pp. 1031-1040.

Wieczorek, U. and **Ivantysynova, M.** 2002. Computer Aided Optimization of Bearing and Sealing Gaps in Hydrostatic Machines - the Simulation Tool CASPAR. *International Journal of Fluid Power*, Vol. 3, No. 1, pp. 7-20.

Monika Ivantysynova
Born on December 11th 1955 in Polenz (Germany). She received her MSc. Degree in Mechanical Engineering and her PhD. Degree in Hydraulics from the Slovak Technical University of Bratislava, Czechoslovakia. After 7 years in fluid power industry she returned to university. In April 1996 she received a Professorship in fluid power & control at the University of Duisburg (Germany). At present she is Professor of Mechatronic Systems at the Technical University of Hamburg-Harburg. Her main research areas are energy saving actuator technology and model based optimisation of displacement machines as well as modelling, simulation and testing of fluid power systems. Besides the book "Hydrostatic Pumps and Motors" published in German and English, she has published more than 60 papers in technical journals and at international conferences

Rolf Lasaar
Born on August 9th 1969 in Mülheim a. d. Ruhr (Germany), study of mechanical engineering at the Gerhard Mercator University of Duisburg, diploma thesis in the area of fuzzy controllers at the Department of Measurement and Control Engineering of Gerhard Mercator University of Duisburg. From 1997 through 2002 research fellow at this department and at the Institute for Aircraft Systems Engineering at the Technical University of Hamburg-Harburg - Doctor degree in 2002. Meanwhile working for Linde AG, Material Handling, Aschaffenburg, Germany